Turkish Journal of Electrical Engineering & Computer Sciences

http://journals.tubitak.gov.tr/elektrik/

Research Article

Turk J Elec Eng & Comp Sci
(2015) 23: 1489 – 1500

doi:10.3906/elk-1307-103

An implementable approach in order to model a nonideal incremental encoder in speed measurement studies

Mahdi MAAREF*, **Alireza REZAZADEH**
School of Electrical and Computer Engineering, Shahid Beheshti University, Iran

Received: 15.07.2013 • **Accepted/Published Online:** 25.09.2013 • **Printed:** 28.08.2015

Abstract: Incremental encoders have attracted significant attention to measure motor speed worldwide. Due to the advantages of incremental encoders a noticeable percentage of Servo system drives have been built based on these sensors. The nonideality of encoders, especially mechanical misalignments, is one of their most important problems, affecting the precision of calculations. In the current paper we present an analytical formula to model the nonideal incremental encoder and calculate both the frequency and magnitude of vibrations due to this nonideality. Moreover, a nonideality identity parameter of the encoder is defined. This parameter can be used for quality assurance purposes. Moreover, it is possible to design flexible filters for measured speed based on this parameter, especially in low resolution encoders. The simulation and experimental results corroborate the precision of the proposed method in a wide range of speeds.

Key words: Nonideal incremental encoder, gap location, encoder resolution, sampling time

1. Introduction

The technology of sensors measuring rotational speed has gained significant attention worldwide. Recent developments in Servo motor drives have heightened the need for using precise sensors and currently it is becoming increasingly difficult to ignore the role of incremental encoders in this field [1–4]. The incremental encoders benefit from accuracy, repeatability, high performance, and flexibility [4–6]. Furthermore, their low price makes them useful in many applications. Despite their safety and efficiency, incremental encoders have several major drawbacks such as limited controller bandwidth in slow speeds, quantization error, and the nonideality effect of the encoder on the measured speed. The debate continues about the best strategies for the manipulation of incremental encoders. More recently many studies have proposed interesting methods in order to eliminate quantization error such as using synchronized pulse counting [7], but the lack of a precise model for a nonideal encoder has been an intricate problem for many years. The objectives of the present research are to determine the behavior of a nonideal encoder and analytically model it. Although synchronized pulse counting eliminates quantization error [8,9], the nonidealities of the incremental encoder can cause fluctuations of the measured speed in steady state conditions [10]. One of the most common nonidealities of the incremental encoder is misalignment and discrepancy of the gap intervals on the encoder's disk due to mechanical errors. Figure 1 depicts the captured speed data of a servo system coupled with an incremental encoder. In both (a) and (b) the motor rotates at a speed of 30 d/s (5 rpm), but in (a) sampling time (T_S) is 0.001s, while in (b) it is 0.01s. By comparing (a) and (b) we observe that a change in T_S corresponds to a change in magnitude and frequency of fluctuations.

*Correspondence: m_maaref@sbu.ac.ir

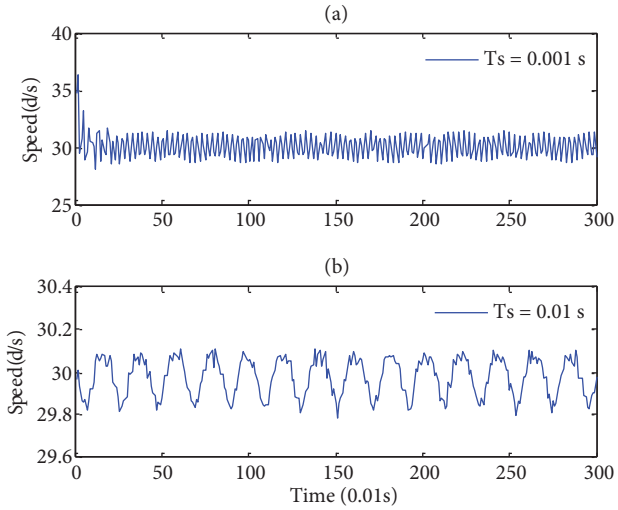

Figure 1. Constant steady state speed in a nonideal encoder. A change in sampling time leads to a change in measured speed. In (a) the real speed is 5 rpm and sampling time equals 0.001 s, the magnitude of vibrations on the measured speed is more than 1 d/s (0.16 rpm). In (b) the real speed is 5 rpm and sampling time equals 0.01 s, the magnitude of vibrations on the measured speed is less than 0.2 d/s (0.03 rpm).

Hence, it can be concluded that the fluctuations in measured speed are dependent not only on motor characteristics but also on incremental encoder nonideality. In order to evaluate the nonideality effect of the encoder on the characterization of these fluctuations (magnitude and frequency), we must assume an ideal motor with a constant rotational speed. In this case the nonideality of the shaft encoder would be the only cause of vibrations. Experimental results show that fast frequency vibrations superimpose on slow-frequency ones, and both depend on sampling time, rotational speed, and encoder resolution. Throughout this paper N_E is used to show the number of encoder's gaps (number of output pulses per 360 degree rotation), Δ_N denotes counted pulses during a synchronized time interval T_M, and ω_r indicates the rotating speed in degree/s.

2. Slow-frequency vibrations

Speed measurement systems can eliminate quantization error by synchronizing sampling time with encoder output pulses. This method is explained in many studies [11] and for an ideal encoder it can measure the rotating speed precisely. Figure 2 shows the output pulse of an encoder.

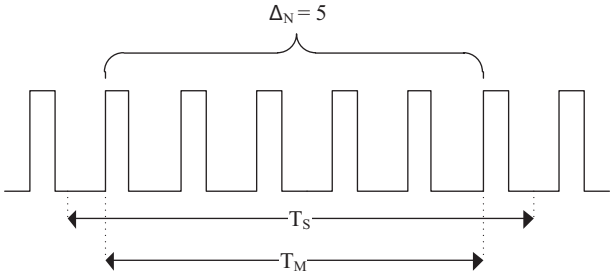

Figure 2. Synchronization of sampling time with output pulses of the encoder.

In Figure 2 T_S indicates sampling time. As it is shown, if during the synchronized sampling time (T_M) the measuring system counts the output pulses (Δ_N), it can calculate the rotating speed using (1) and (2):

$$\Delta_\theta = \frac{\Delta_N \times 360}{N_E} \tag{1}$$

$$\omega_r = \frac{\Delta_\theta}{\Delta_t} = \frac{\Delta_\theta}{T_M} = \frac{360.\Delta_N}{N_E.T_M} \tag{2}$$

Figure 3 shows an encoder that rotates at a speed of ω_r and a sampling time of T_S and so the number of counted pulses per T_S can be calculated as

$$\Delta_N = \frac{\omega_r \times T_M \times N_E}{360} = \left\lfloor \frac{\omega_r \times T_S \times N_E}{360} \right\rfloor \tag{3}$$

where $\lfloor x \rfloor$ indicates the largest integer smaller than or equal to x.

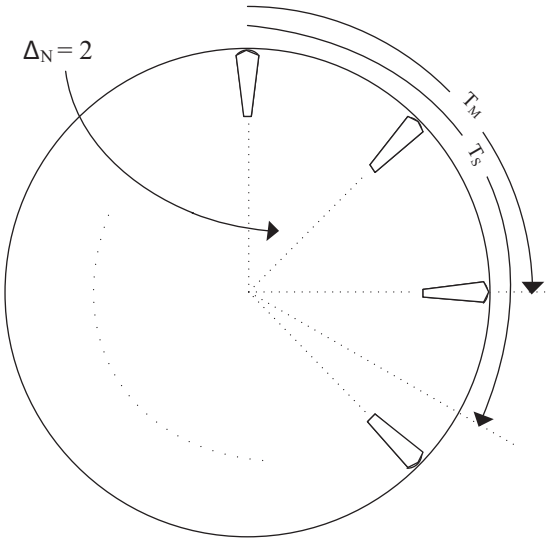

Figure 3. Calculating Δ_N based on T_S, ω_r and N_E.

In order to calculate the slow-frequency vibrations we present the term "Round Number" or R_N. Figure 4 shows a simple encoder with 9 gaps. We assume that each gap represents a state and so we have 9 states. If we assume that we start moving from state number one and in each movement we pass Δ_N states through the encoder disk, after R_N movements we will get to state number one again. Therefore, the value of R_N depends on both N_E and Δ_N. Mathematically, R_N can easily be calculated as follows:

$$R_N = \frac{LCM(N_E, \Delta_N)}{N_E} = \frac{LCM(N_E, \lfloor \frac{\omega_r \times T_S \times N_E}{360} \rfloor)}{N_E} \tag{4}$$

where LCM(x, y) is the least common multiple of x and y. In order to clarify the problem, a numerical example has been explained based on the encoder shown in Figure 4.

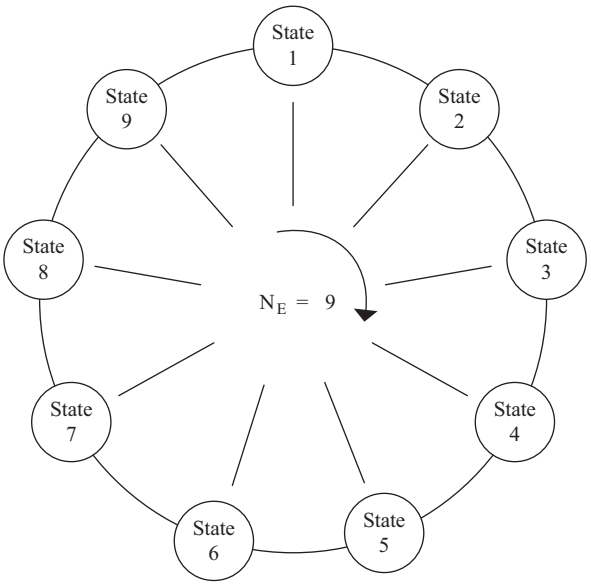

Figure 4. An example encoder in order to evaluate slow frequency vibrations.

If Δ_N equals 6, after the first T_S we move from state 1 to state 7. In the second T_S we move from state 7 to state 4, and in the third T_S we move from state 4 to state 1. Therefore, in this example Round Number (R_N) equals 2 because we rotate 720 degree (2×360) before arriving at the first state. Table 1 shows the calculated R_N and transient states for different values of Δ_N in the above example. After arriving at the first state it is obvious that this chain repeats periodically, and so if we measure the time interval between the two periods we can calculate the frequency of the slow fluctuations. Using (2) we can write:

$$f_{slow-fluc} = \frac{1}{360 \times \omega_r \times R_N} \tag{5}$$

Based on (4), the slow-frequency of the encoder's fluctuations can be calculated as follows:

$$f_{slow-fluc} = \frac{N_E}{360 \times \omega_r \times LCM(N_E, \lfloor \frac{\omega_r \times T_S \times N_E}{360} \rfloor)} \tag{6}$$

Table 1. Calculating R_N and transient states for different values of Δ_N.

Δ_N	**1**	**2**	**3**	**4**	**5**	**6**	**7**	**8**	**9**
Transient states	1	1	1	1	1	1	1	1	1
	2	3	4	5	6	7	8	9	1
	3	5	7	9	2	4	6	8	
	4	6	1	4	7	1	4	7	
	5	9		8	3		2	6	
	6	2		3	8		9	5	
	7	4		7	4		7	4	
	8	6		2	9		5	3	
	9	8		6	5		3	2	
	1	1		1	1		1	1	
R_N	1	2	1	4	5	2	7	8	1

3. Fast-frequency of fluctuations

Experimental results show that the frequency of fast vibrations of the measured speed is not perfectly constant and these fluctuations have disorganized behavior. Therefore, in order to evaluate the frequency of fast-vibrations it is important to consider the actual location of each gap through the encoder disk. Figure 5 shows a nonideal incremental encoder with 8 gaps per round ($N_E = 8$). For each gap a nominal and actual location has been depicted. In addition, we assume that the encoder rotates ideally at a speed of 45 d/s.

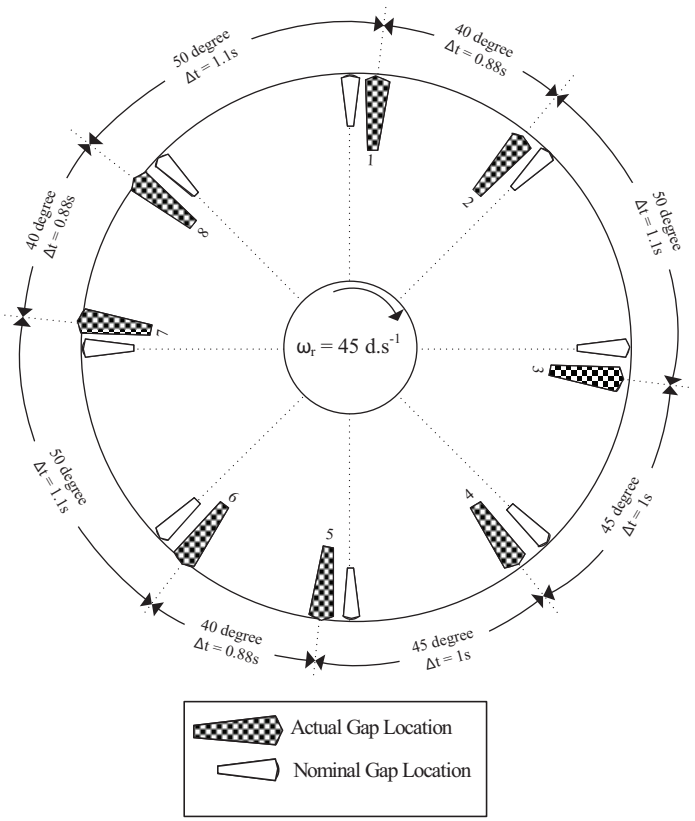

Figure 5. Actual and nominal locations of gaps on the encoder's disk with $N_E = 8$.

As seen from Figure 5, the nominal distance between gaps 1 and 2 is 45 degrees, while the actual distance between them is 40 degrees. Using (2), the time interval between these two gaps can be calculated as follows:

$$\Delta_t = \frac{\Delta_\theta}{\omega_r} \Rightarrow \Delta_t = \frac{40}{45} = 0.88s \tag{7}$$

Now we can calculate the measured speed (ω_m) easily as follows:

$$\omega_m = \frac{\Delta_\theta}{\Delta_t} \Rightarrow \omega_m = \frac{45}{0.88} = 51.13d.s^{-1} \tag{8}$$

By comparing Eqs. (7) and (8), the error of the speed measurement (Δ_ω) due to nonideality of the encoder has been obtained:

$$\Delta_\omega = |\omega_r - \omega_m| = |45 - 51.13| = 6.13d.s^{-1} \tag{9}$$

where $|x|$ shows the absolute value of x. Figure 6 represents the repetition of this procedure for different values of sampling time (T_S).

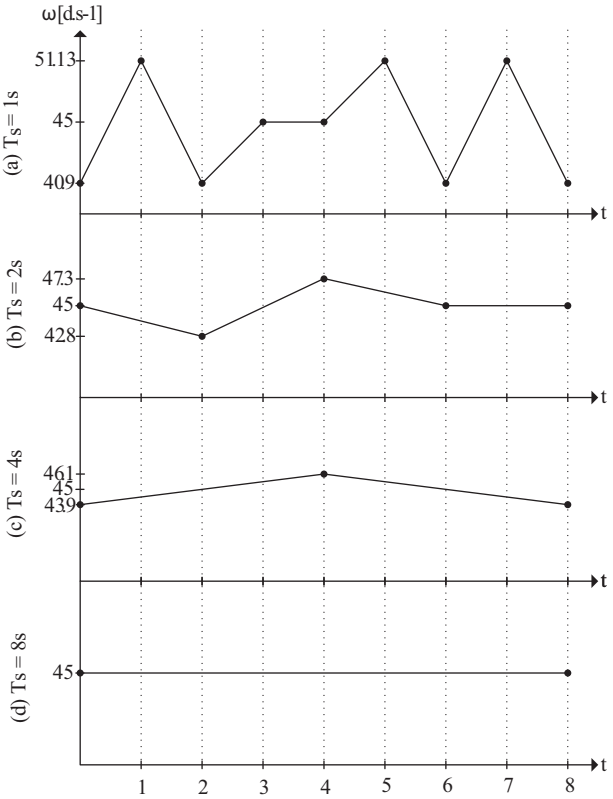

Figure 6. The measured speed for different values of sampling time by means of a nonideal encoder.

As seen from Figure 6, the frequency of fast vibrations of the measured speed was decreased by increasing the sampling time. As shown in Figure 6 part (d), if the multiplication of sampling time and real speed equals 360, after one T_S the encoder sees the first gap again and the nonideality of the other gaps does not influence calculations. It means that in this condition the measurement error equals zero.

$$T_S \times \omega_r = 8 \times 45 = 360 \Rightarrow \omega_r = \omega_m = 45 d.s^{-1} \tag{10}$$

The frequency of fast fluctuations is obtained based on Figure 6 and Eq. (2) as follows:

$$f_{fast-fluc} = \frac{1}{2.T_M} = \frac{1}{2 \times \frac{360.\Delta_N}{N_E.\omega_r}} \tag{11}$$

From (3) we have

$$f_{fast-fluc} = \frac{\omega_r \times N_E}{720 \times \left\lfloor \frac{\omega_r \times T_S \times N_E}{360} \right\rfloor} \tag{12}$$

4. Magnitude of fluctuations

As depicted in Figure 6, changing the sampling time will change the magnitude of vibrations. However, vibration magnitude also depends on another important variable, θ_{fault}, which denotes the angle between the nominal

and actual location of each gap on the encoder's disk. Figure 7 shows θ_{fault} for one gap. It is undeniable that in a real incremental encoder each gap has its own θ_{fault}, but obviously it can be a complicated procedure to measure θ_{fault} separately for each gap, especially in high resolution encoders. Therefore, in this paper we assume θ_{fault} as a normal random variable with a mean value of zero and a standard deviation of σ as follows:

$$\theta_{fault} \sim \mathrm{N}(0, \sigma^2) \tag{13}$$

This distribution is often used in natural and social sciences for real-value random variables whose distribution is totally unknown [12]. Therefore, we can conclude that σ indicates the precision of the mechanical design and construction of the encoder.

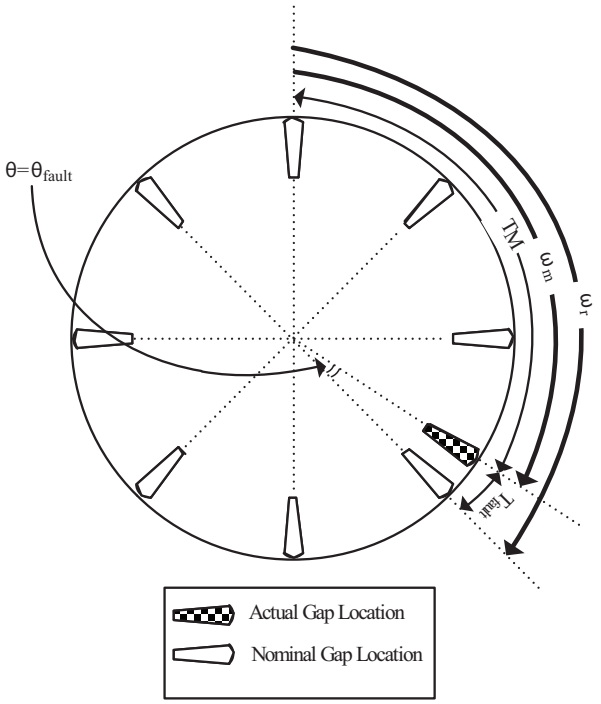

Figure 7. Angle between the nominal and actual locations of each gap on the encoder disk.

As seen from Figure 7, real and measured speeds are calculated respectively as follows:

$$\omega_r = \frac{360.\Delta_N}{N_E.(T_M + T_{fault})} \tag{14}$$

$$\omega_m = \frac{360.\Delta_N}{N_E.T_M} \tag{15}$$

In Eq. (15) , T_{fault} denotes the time interval between the actual and nominal location of a gap when the encoder rotates at ω_r speed. Therefore, we can write

$$T_{fault} = \frac{\theta_{fault}}{\omega_r} \tag{16}$$

From (14) and (16) we have

$$\omega_r = \frac{360.\Delta_N}{N_E.(T_M + \frac{\theta_{fault}}{\omega_r})} \tag{17}$$

Thus, the ratio of ω_m to ω_r be equal to

$$\frac{\omega_m}{\omega_r} = \frac{\frac{1}{T_M}}{\frac{1}{T_M + \frac{\theta_{fault}}{\omega_r}}} = 1 + \frac{\theta_{fault}}{T_M.\omega_r} \tag{18}$$

This will lead to

$$\Delta_\omega = |\omega_m - \omega_r| = \frac{\theta_{fault}}{T_M} \tag{19}$$

Eq. (19) shows that the measurement error depends on both the standard deviation of the encoder and the measuring time. For an ideal encoder, the standard deviation goes to zero and so Δ_ω is infinitely small. For a nonideal encoder, if we allocate high values for T_M, we can decrease the error based on (19). Now, in order to calculate the value of Δ_ω we can use (11) and so

$$\Delta_\omega = 2 \times \theta_{fault} \times f_{fast-fluc} \tag{20}$$

As we mentioned before, θ_{fault} is a normal random variable with a mean value of zero and a standard deviation of σ. Therefore, the absolute moments of θ_{fault} are written as

$$E(|X|^p) = \sigma^p . \frac{2^{\frac{p}{2}} \times \Gamma(\frac{p+1}{2})}{\sqrt{\pi}} \tag{21}$$

where p is the order of the absolute moments and $\Gamma(x)$ denotes the Gamma function. In this article we use the first order of absolute moment ($p = 1$). Thus, we can calculate the absolute expected value of θ_{fault} as follows:

$$E(|X|) = \sigma\sqrt{\frac{2}{\pi}} \tag{22}$$

and we can rewrite (20) as follows:

$$\Delta_\omega = 2\sqrt{\frac{2}{\pi}} \times \sigma \times f_{fast-fluc} \tag{23}$$

From (12), Δ_ω is obtained as

$$\Delta_\omega = \frac{\sqrt{2}\sigma.\omega_r.N_E}{360\sqrt{\pi} \times \lfloor \frac{\omega_r \times T_S \times N_E}{360} \rfloor} \tag{24}$$

5. Simulation results

In order to simulate the proposed method, a Matlab/Simulinx program is developed. In this program an ideal incremental encoder with N_E pulses per round is simulated as follows:

$$A(\theta) = \begin{cases} 1 & \theta \in GAPS \\ 0 & Otherwise \end{cases} \tag{25}$$

where $A(\theta)$ is a function of the encoder's output pulses and $GAPS$ is defined as a set of angles that demonstrate the place of encoder gaps. For example, for an encoder with N_E gaps we have

$$GAPS \equiv \left\{ \frac{0 \times 360}{N_E}, \frac{1 \times 360}{N_E}, \frac{2 \times 360}{N_E}, ..., \frac{(N_E - 1) \times 360}{N_E} \right\} \tag{26}$$

Now, based on Eqs. (25) and (26) we can model a nonideal encoder easily. It is enough to modify GAPS sets as follows:

$$GAPS \equiv \left\{ \frac{0 \times 360}{N_E} + a_0, \frac{1 \times 360}{N_E} + a_1, \frac{2 \times 360}{N_E} + a_2, ..., \frac{(N_E - 1) \times 360}{N_E} + a_n \right\} \tag{27}$$

where $\alpha_i \sim \mathrm{N}(0, \sigma^2)$. Figures 8 and 9 show the results. In this simulation we assumed $N_E = 10,000$, $\sigma = 0.005$, $T_S = 0.01s$, and $\omega_r = 5d/s$. We used large scale zoom in order to see both slow and fast frequency vibrations in Figure 8. Figure 9 shows the simulation and the proposed method results. As can be seen, the precision of the frequency calculation by the proposed method is very good. We repeat the simulations for different values of T_S and σ in order to gain a comprehensive comparison between simulation and the proposed method results presented in Tables 2 and 3. Table 2 shows the calculated measures of fast frequency vibrations for different amounts of T_S and under the assumption of constant N_E, σ, and ω_r. It can be seen that in the worst case there is only 0.08% error in detecting the frequency of fast fluctuations. Similarly, in Table 3 we present the amounts of vibration magnitude calculated using the proposed method under the assumption of constant N_E, T_S, ω_r, and for different values of σ. In this case the worst case estimation error would be 0.22%, which is still quite precise.

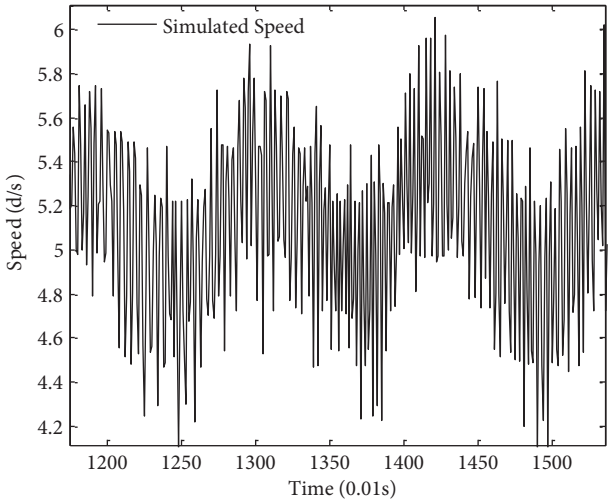

Figure 8. Both low and fast fluctuations.

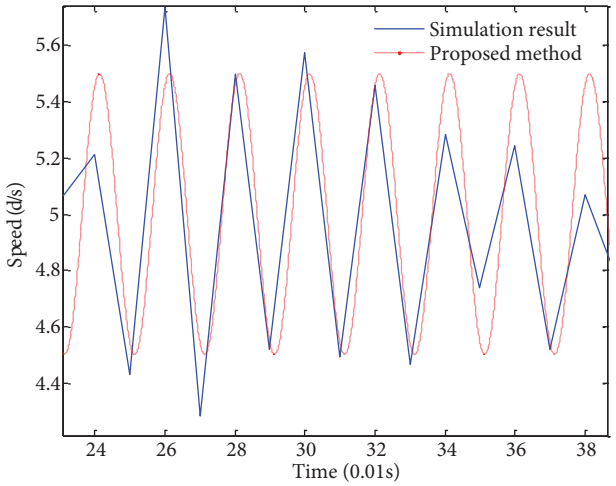

Figure 9. Comparison between simulation results and the proposed method results.

Table 2. Comparison between simulation results and the proposed method results for fast frequency vibrations. For the case of $\sigma = 0.005$ and $\omega_r = 50d/s$.

T_S	Simulation results of frequency	Proposed method results of frequency	Error
0.001 s	688.3 Hz	694.44 Hz	0.00892%
0.05 s	11.03 Hz	10.0644 Hz	0.08754%
0.01 s	54.82 Hz	53.41 Hz	0.02572%
0.1 s	5.29 Hz	5.03 Hz	0.04914%

6. Experimental study

In this study the experimental approach is developed in two totally different stages. First, we propose a method in order to calculate σ for any desired incremental encoder. Then we run the motor in different steady-state speeds and evaluate the accuracy of the proposed method by comparing fluctuations that are calculated both experimentally and analytically.

Table 3. Magnitude vibrations comparison between simulation results and the proposed method results in the case of $N_E = 10,000, \omega_r = 35d/s$, and $T_S = 0.05$.

σ	Simulation results of Δ_ω	Proposed method results of Δ_ω	**Error**
0.001	0.021 (d/s)	0.0162 (d/s)	0.2285%
0.03	0.5324 (d/s)	0.4848 (d/s)	0.0894%
0.95	14.2391 (d/s)	15.3530 (d/s)	0.0782%

7. Calculating σ for any desired incremental encoder

The main goal of this approach is to calculate σ as a quantity to identify the ideality of an incremental encoder. In other words, we define σ as an identification parameter of the encoder. This parameter can be used for quality assurance purposes and for designing a filter for the measured speed.

In this experimental test we use a low resolution encoder as a desired encoder whose σ must be calculated, and a high resolution encoder as an ideal reference one. Therefore, we assembled an NSK direct drive servo system (with internal 1,200,000 reference encoder) and an FPGA based controller (Figure 10). The synchronized speed measurement method is implemented in Xilinx Spartan 3E FPGA. The source code is written in Verilog language and a TCP/IP Ethernet protocol is used aimed at real time data transportation. Then a low resolution encoder with 3600 pulses per round was coupled to the rotor. The goal was to calculate the σ parameter for this encoder.

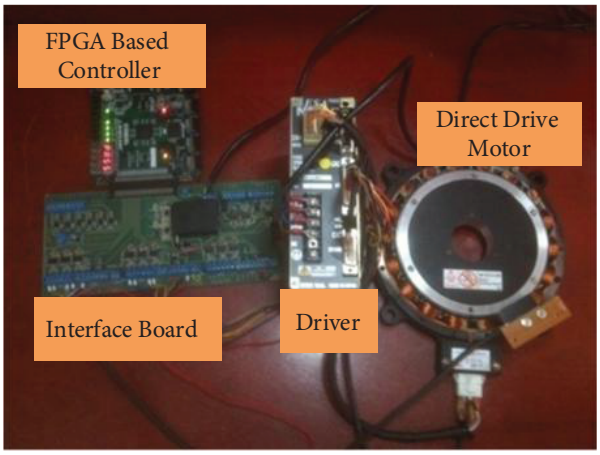

Figure 10. A case study including an NSK direct drive servo system and an FPGA based controller.

After running the motor at a speed of 20 d/s (3.3 rpm) and reaching a steady-state speed we calculated the real speed (ω_r) using a reference high resolution encoder (1,200,000 pulses per round). In this test T_S was set to 0.01 s. Then we measured the speed using a low resolution encoder and calculated the magnitude of vibrations (Δ_ω). Both ω_r and Δ_ω are depicted in Figure 11. In Figure 11 ω_r is shown in red and Δ_ω is

shown in blue. Based on these results, ω_r and Δ_ω are equal to 19.78 d/s (3.29 rpm) and 0.63 d/s (0.105 rmp) respectively.

Now, regarding Eq. (24), it is easy to find the value of σ.However, it is important to mention that N_E in this equation is 3600 instead of 1,200,000 because we want to calculate the σ parameter for a low resolution encoder. Therefore, using (24), the σ value is calculated as 0.0041.

8. Evaluating the accuracy of the proposed method

In order to evaluate the accuracy of the presented method, we run the motor in different steady-states speeds and compare experimental and analytical values ofΔ_ω. Figure 12 and Table 4 show the results, which indicate that the proposed method benefits from stability and accuracy during different ranges of steady-state speeds. These results validate the precision of the analytical calculations proposed in this approach.

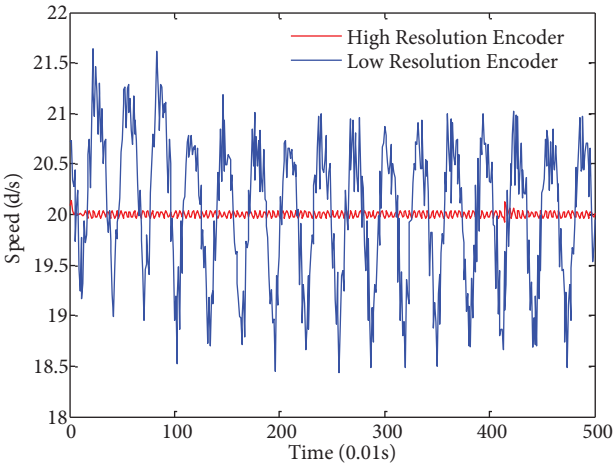

Figure 11. Measured speed of low and high resolution encoders.

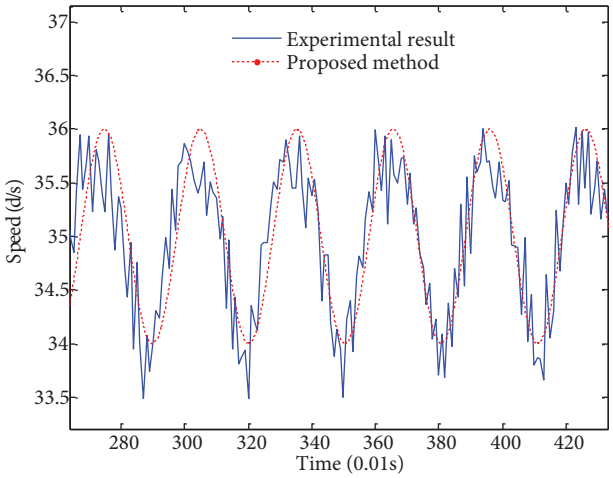

Figure 12. Experimental results in steady states.

Table 4. Experimental results under different steady-state motor speeds.

ω_r	Experimental results of Δ_ω	Proposed method results of Δ_ω	**Error**
1.6 rpm	0.052 rpm	0.054 rpm	0.03852%
4.16 rpm	0.0687 rpm	0.0681 rpm	0.00807%
9.16 rpm	0.062 rpm	0.0599 rpm	0.03751%
12.5 rpm	0.056 rpm	0.058 rpm	0.032525%

9. Conclusion

In this paper we developed analytical calculations in order to model a nonideal incremental encoder. First we proved experimentally that some parts of vibrations in the measured speed are due to nonideality of the encoder. Then we modelled the nonideal incremental encoder and calculated the frequency and magnitude of vibrations separately. Parameter σ was defined in order to identify the nonideality of an encoder and calculate the magnitude of fluctuations sampling time (N_E), rotational speed (ω_r), and encoder resolution (N_E). This parameter denotes the merit gauge of an encoder and can be used for many purposes. As a case in point, we can design flexible filters for output speed due to the fact that at any speed the characterization of speed error

is known. In order to validate the proposed method, both simulation and experimental evaluations were used. The results show that the presented algorithm is valid in a wide ranges of speeds and reaches accurate and stable responses while dealing with low level calculations.

List of Abbreviations and Symbols

Δ_N	Counted pulses in one sampling time.
Δ_θ	Rotated angle in degrees.
N_E	Number of encoder's gaps per 360 degrees.
Δ_t	Time interval between two events in seconds.
T_M	Measured time synchronized with encoder's output pulses.
T_S	Sample time.
R_N	Round Number (number of rounds that must go through the circle in order return to the first state).
$f_{slow-fluc}$	Frequency of slow fluctuations.
$f_{fast-fluc}$	Frequency of fast fluctuations.
T_{fault}	Time interval between nominal and actual gaps.
Δ_ω	Magnitude of fluctuations ($\lvert\omega_m - \omega_r\rvert$).

References

[1] Johnson N, Mohan KJ, Janson KE, Jose J. Optimization of incremental optical encoder pulse processing. In: IEEE 2013 International Multi-Conference on Automation, Computing, Communication, Control, and Compressed Sensing (iMac4s); 22–23 March 2013; Kottayam, India: IEEE. pp. 769–773.

[2] Negrea AC, Imecs M, Incze II, Pop A, Szabo, C. Error compensation methods in speed identification using incremental encoder. In: IEEE 2012 International Conference and Exposition on Electrical and Power Engineering (EPE); 25–27 October 2012; Iasi, Romania: IEEE. pp. 441–445.

[3] Abdagic A, Sinanovic A, Velagic J, Osmic N. Reduction of low-resolution incremental encoder usage effects on control performance by using a fuzzy controller. In: IEEE 2011 International Symposium on Information, Communication, and Automation Technologies (ICAT); 27–29 October; Sarajevo, Bosnia and Herzegovina: IEEE. pp. 1–6.

[4] Negrea CA, Incze, II, Imecs M, Pop AV, Szabo C. An improved speed identification method using incremental encoder in electric drives. In: IEEE 2012 International Conference on Automation Quality and Testing Robotics (AQTR); 24–27 May 2012; Cluj-Napoca, Romana: IEEE. pp. 536–540.

[5] Arabaci H, Bilgin O. A novel motor speed calculation method using square wave speed sensor signals via fast Fourier transform. Turk J Elec Eng & Comp Sci 2012; 20: 1090–1099.

[6] Merry RJE, Molengraft MJG, Steinbuch M. Velocity and acceleration estimation for optical incremental encoders. Mechatronics 2010; 20: 20–26.

[7] Petrella R, Tursini M. An embedded system for position and speed measurement adopting incremental encoders. IEEE Trans. on Industry Applications 2008; 44: 1436–1444.

[8] Mohan JK, Johnson N. Devising Simulink Optical Encoder Pulse Manipulation and its Evaluation. In: IEEE 2012 International Conference on Intelligent Systems Design and Applications (ISDA): 27–29 November 2012; Kochi, India: IEEE . pp. 640–644.

[9] Maaref M, Rezazadeh A, Shokouhandeh H. An implementable speed measurement method in order to eliminate quantization error while using rotary incremental encoders. Journal of Basic and Applied Scientific Research (JBASR) 2013; 3: 7–19.

[10] Kavanagh RC. Shaft encoder characterization through analysis of the mean-squared errors in nonideal quantized systems. IEE Proceedings of Science, Measurement and Technology 2002; 149: 99–104.

[11] Chow HW, Cheung N. High Speed Processing of Encoder Information by Using a Dual-resolution Approach. In IEEE 2010 Conference on Industrial Electronics and Applications (ICIEA); 15–17 June 2010; Taichung, Republic of China: IEEE. pp. 644–649.

[12] Torres-Trevio LM. On the Estimation of the Pareto Optimal Set Using an Evolutionary Parameter Adjustment of the Normal Distribution Function. In: IEEE 2008 Artificial Intelligence Mexican International Conference; 27–31 October 2008; Atizapan de Zaragoza, Mexico: IEEE. pp. 176–181.